Inorg. Chem. **2005**, *44*, 4616–4621

Synthesis and Molecular and Extended Structures for a Diaminonaphthalene-Derived Bis(amido)stannylene

Patrick Bazinet,[†] Glenn P. A. Yap,[†] Gino A. DiLabio,*[,‡] and Darrin S. Richeson*[,†]

Department of Chemistry, University of Ottawa, Ottawa, Ontario, Canada K1N 6N5, and National Institute for Nanotechnology, National Research Council of Canada, W6-010 ECERF, 9107-116th Street, Edmonton, Alberta, Canada T6G 2V4

Received February 15, 2005

The cyclic bis(amido)tin(II) compound Sn[1,8-(^{i}PrN)$_2$C$_{10}$H$_6$] (**2**) was isolated from the reaction of Li$_2$[1,8-(^{i}PrN)$_2$C$_{10}$H$_6$] (**1**) and SnCl$_2$. Solid-state structural analysis of **2** showed it to be a mononuclear species with a pyramidal Sn center as part of a nonplanar metallaheterocycle. The packing diagram of **2** revealed an extended one-dimensional head-to-tail chain structure with short intermolecular Sn/arene-C interactions. Computational examination of **2** (DFT/PW91 and MP2 with 6-31G* and 6-311G** basis functions) indicated that the optimum gas-phase structure of **2,** which displays a Sn center in the plane of the naphthyl backbone with a slightly twisted metallaheterocycle, is approximately 24 kcal/mol lower in energy than the X-ray structure. The solid-state geometry of **2** is attributed to the intermolecular donation of the naphthalene π-electrons to a Lewis acidic Sn center, which leads to the observed supramolecular structure. The crystal structure of **1** is also reported.

Introduction

Divalent compounds of the heavier group 14 elements represent potential building blocks for synthetic chemistry of these elements and have attracted interest from fundamental and applied perspectives.[1−3] Amido ligands continue to play a pivotal role in advancing this field and have been employed for the isolation and characterization of mononuclear, thermally stable M(II) (M = Si, Ge, Sn) complexes with the archetypes being M(N(SiMe$_3$)$_2$)$_2$ (M = Ge, Sn, Pb).[4] Theoretical and experimental results indicate that anionic, nitrogen-based ligands lend stability to these species through a combination of a σ-inductive effect and π-donation with further stability provided by ligand frames that possess a delocalized heterocyclic π-system.[5] The role of delocalization likely declines as one moves down the period. In addition, the presence of sterically demanding substituents on the metal-bonded nitrogen centers undoubtedly plays an essential role in preventing aggregation of these species.[6]

Our general interests in the design and implementation of rigid chelating ligands with delocalized π-electrons led us to prepare the diamido ligand **A**. This species is derived from 1,8-diaminonaphthalene (DAN) and should yield a six-membered metallaheterocycle when coordinated to a metal

* To whom correspondence should be addressed. E-mail: darrin@science.uottawa.ca (D.S.R.), Gino.DiLabio@nrc-cnrc.gc.ca (G.A.D.).
† University of Ottawa.
‡ National Research Council of Canada.

(1) Hill, N. J.; West, R. *J. Organomet. Chem.* **2004**, *689*, 4165.
(2) Kuhl, O. *Coord. Chem. Rev.* **2004**, *248*, 411.
(3) For selected recent examples, see: Fedushkin, I. L.; Skatova, A. A.; Chudakova, V. A.; Khvoinova, N. M.; Baurin, A. Y.; Deckert, S.; Hummert, M.; Schumann, H. *Organometallics* **2004**, *23*, 3714. Jing, H.; Edulji, S. K.; Gibbs, J. M.; Stern, C. L.; Zhou, H.; Nguyen, S. T. *Inorg. Chem.* **2004**, *43*, 4315. Hitchcock, P. B.; Hu, J.; Lappert, M. F.; Severn, J. R. *Dalton Trans.* **2004**, 4193. Richards, A. F.; Brynda, M.; Power, P. P. *Organometallics* **2004**, *23*, 4009.
(4) (a) Schaeffer, C. D., Jr.; Zuckerman, J. J. *J. Am. Chem. Soc.* **1974**, *96*, 7160. (b) Harris, D. H.; Lappert, M. F. *J. Chem. Soc., Chem. Commun.* **1974**, 895. (c) Gynane, M. J. S.; Harris, D. H.; Lappert, M. F.; Power, P. P.; Rivière, P.; Rivière-Baudet, M. *J. Chem. Soc., Dalton Trans.* **1977**, 2004. (d) Chorley, R. W.; Hitchcock, P. B.; Lappert, M. F.; Leung, W.-P.; Power, P. P.; Olmstead, M. M. *Inorg. Chim. Acta* **1992**, *198*−*200*, 203. (e) Fjeldberg, T.; Hope, H.; Lappert, M. F.; Power, P. P.; Thorne, A. J. *J. Chem. Soc., Chem. Commun.* **1983**, 639.
(5) Lehmann, J. F.; Urquhart, S. G.; Ennis, L. E.; Hitchcock, A. P.; Hatano, K.; Gupta, S.; Denk, M. K. *Organometallics* **1999**, *18*, 1862. Hermann, W. A.; Köcher, C. *Angew. Chem., Int. Ed. Engl.* **1997**, *36*, 2162. Boehme, C.; Frenking, G. *J. Am. Chem. Soc.* **1996**, *118*, 2039. Heinemann, C.; Müller, T.; Apeloig, Y.; Schwarz, H. *J. Am. Chem. Soc.* **1996**, *118*, 2023. Driess, M.; Grützmacher, H. *Angew. Chem., Int. Ed. Engl.* **1996**, *35*, 828. Denk, M.; Lennon, R.; Hayashi, R.; West, R.; Beyakov, A. V.; Verne, H. P.; Haaland, A.; Wagner, M.; Metzler, N. *J. Am. Chem. Soc.* **1994**, *116*, 2691. Heinemann, C.; Hermann, W. A.; Theil, W. *J. Organomet. Chem.* **1994**, *475*, 73. Hermann, W. A.; Denk, M.; Behm, J.; Scherer, W.; Klingan, F. R.; Bok, H.; Solouki, B.; Wagner, M. A*ngew. Chem., Int. Ed. Engl.* **1992**, *31*, 1485. Pfeiffer, J.; Maringgele, W.; Noltemeyer, M.; Meller, A. *Chem. Ber.* **1989**, *122*, 245.
(6) Denk, M. K.; Thadani, A.; Hatano, K.; Lough, A. J. *Angew. Chem., Int. Ed. Engl.* **1997**, *36*, 2607.

10.1021/ic050238u CCC: $30.25
Published on Web 05/26/2005

center.[7,8] We recently employed **A** in the preparation of the Ge compound Ge[1,8-(^{i}PrN)$_2$C$_{10}$H$_6$], **B**,[9] and have used this scaffold for the isolation of a novel carbene **C**.[10] We now report the synthetic and structural details for a new stannylene compound supported by this ligand, Sn[1,8-(^{i}PrN)$_2$C$_{10}$H$_6$]. Two related ligands have been employed for the isolation of Sn(II) species.[4a,11] The structural characterization of the dilithium salt of **A** (R = ^{i}Pr), a useful precursor to this and other metal amido species, is also presented.

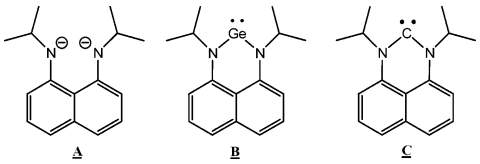

A **B** **C**

Experimental Section

General Methods. All manipulations were carried out in either a nitrogen-filled drybox or under nitrogen using standard Schlenk-line techniques. Unless otherwise noted, solvents were sparged with nitrogen and then dried by passage through column of activated alumina using an apparatus purchased from Anhydrous Engineering. Deuterated benzene and toluene were dried by vacuum transfer from potassium. $SnCl_2$ and 1,8-diaminonaphthalene were purchased from Aldrich and used without further purification. ^{1}H NMR spectra were run on either a Gemini 200 MHz or a Bruker 500 MHz spectrometer with deuterated benzene or toluene as a solvent and internal standard. All elemental analyses were run on a Perkin-Elmer PE CHN 4000 elemental analysis system.

Computational Methods. Hydrogen-atom-only optimizations of the crystal structure of **2** as well as full geometry optimizations were carried out using the PW91 density functional. Tin was represented with averaged relativistic core potentials[12] (4d, 5s, and 5p subshells in the valence space) with the recommended basis set (3s3p4d) used fully uncontracted. The remaining atoms were represented with 6-31G* basis sets. Single-point energies were computed at the PW91 minima using the MP2 approach. Additional optimizations were performed with PW91 with a 3s3p4d1f basis set for tin and 6-311G** bases for the remaining atoms.

Preparation of 1,8-(^{i}PrNH)$_2$C$_{10}$H$_6$. To a Teflon screw cap-sealed flask was added 1,8-diaminonaphthalene (5.0 g, 31.6 mmol), activated molecular sieves (5.0 g), and acetone (18.5 g, 319 mmol). The reaction was heated to 80 °C overnight. The reaction mixture was filtered, and the solids were washed with diethyl ether. The ether solutions were combined, and all volatiles were removed under vacuum to give 5.87 g of a red/purple solid that we have preliminarily identified as the aminal 2,2-dimethyl-2,3-dihydroperimidine. This solid (5.0 g, 25.2 mmol) was dissolved in diethyl ether and added dropwise to a suspension of $LiAlH_4$ (2.9 g, 76 mmol) in 100 mL of diethyl ether that was maintained at 0 °C. After addition, the reaction was allowed to warm to room temperature and stirred for an additional 12 h. The reaction was then quenched, at 0 °C, with 2-propanol followed by water. This mixture was extracted with diethyl ether and dried under vacuum to give a purple oil (4.12 g). Following the procedure described above, the oil from this step (1.0 g) was allowed to react with acetone (5.8 g, 100 mmol) to yield 0.83 g of purple oil. This material (3.0 g) was further reacted with $LiAlH_4$ (1.2 g, 32 mmol) using the process described above. A similar isolation procedure led to the isolation of the target product as a purple oil (2.1 g, 70%). This product can be purified by silica gel column chromatography using hexanes as the eluent.

^{1}H NMR ($CDCl_3$, 500 MHz): δ 7.19−7.24 (m, 4H, C*H*), 6.58 (m, 2H, C*H*), 5.63, (br, 2H, N*H*), 3.58 (sept, 2H, C*H*Me$_2$), 1.24 (d, 12H, C*H*$_3$). ^{13}C NMR ($CDCl_3$, 500 MHz): δ 145.0 (*C*), 137.3 (*C*), 125.9 (*C*H), 119.3 (*C*H), 117.9 (*C*), 110.3 (*C*H), 46.4 (*C*HMe$_2$), 22.6 (*C*H$_3$).

Preparation of Li$_2$[1,8-(^{i}PrN)$_2$C$_{10}$H$_6$](THF)$_4$ (1). Addition of MeLi (2.5 mL, 1.4 M in ether, 3.5 mmol) to a stirring dark red/purple solution of 1,8-(^{i}PrNH)$_2$C$_{10}$H$_6$ (0.424 g, 1.7 mmol) in ether (ca. 30 mL) led to an immediate color change of the solution to green then brown with gas evolution. The reaction mixture was stirred for 4 h, and then all volatiles were removed under vacuum. The crude product (0.440 g, 99%) was then purified by crystallization from THF at −35 °C. The crystals were filtered and dried under vacuum (0.830 g, 90%). ^{1}H NMR (C_6D_6): δ 7.40 (t, 2H, Ar-H), 6.94 (d, 2H, Ar-H), 6.36 (m, 2H, Ar-H), 3.55 (sept, 2H, CH(Me)$_2$), 3.36 (t, 16H THF) 1.28−1.18 (overlapping signals, 28H, CH_3 and THF). ^{13}C NMR (C_7D_8, 500 MHz): δ 150 (*C*), 139.5 (*C*), 127.1 (*C*H), 110.9 (*C*H), 115.0 (*C*) 101.3 (*C*H), 68.0 (*C*H$_2$, THF), 47.3 (*C*HMe$_2$), 25.6 (*C*H$_2$, THF), 25.1 (*C*H$_3$). Anal. Calcd for $C_{32}H_{52}N_2O_4Li_2$: C, 70.83; H, 9.66; N, 5.16. Found: C, 70.48; H, 9.29; N, 5.50.

Preparation of Sn[1,8-(N(CH(CH$_3$)$_2$)C$_{10}$H$_6$] (2). To a solution of 1,8-(^{i}PrNH)$_2$C$_{10}$H$_6$ (0.485 g, 2.0 mmol) in 30 mL of diethyl ether was added sequentially MeLi (2.86 mL, 4.0 mmol) followed by $SnCl_2$ (0.378 g, 2.0 mmol). After the reaction mixture was stirred for 8 h, the solvent was evaporated under vacuum and extracted with toluene to yield **2** (0.561 g, 78%). The product could be further purified by recrystallization from hot toluene. ^{1}H NMR (C_7D_8, 500 MHz): δ 7.24 (t, 2H, C*H*), 7.15 (d, 2H, C*H*), 6.32 (d, 2H, C*H*), 4.05 (sept, 2H, C*H*Me$_2$), 1.27 (d, 12H, C*H*$_3$). ^{13}C NMR (C_7D_8, 500 MHz): δ 149.1 (*C*), 139.0 (*C*), 126.3 (*C*H), 118.7 (*C*H), 116.8 (*C*), 105.3 (*C*H), 51.8 (*C*HMe$_2$), 27.8 (*C*H$_3$). ^{119}Sn NMR (C_7D_8, 500 MHz): δ 330 (br). Anal. Calcd for $C_{16}H_{20}N_2Sn$: C, 53.52; H, 5.61; N, 7.80. Found: C, 53.87; H, 5.62; N, 7.73.

Structural Determinations for 1 and 2. Single crystals were mounted on thin glass fibers using viscous oil and then cooled to the data collection temperature. Crystal data and details of the measurements are summarized in Table 1. Data were collected on a Bruker AX SMART 1k CCD diffractometer using 0.3° ω-scans at 0, 90, and 180° in ϕ. Unit-cell parameters were determined from 60 data frames collected at different sections of the Ewald sphere. Semiempirical absorption corrections based on equivalent reflections were applied.

The structures were solved by direct methods, completed with difference Fourier syntheses, and refined with full-matrix least-squares procedures on the basis of F^2. All non-hydrogen atoms were refined with anisotropic displacement parameters. All hydrogen

(7) Lee, C. H.; La, Y.-H.; Park, J. W. *Organometallics* **2000**, *19*, 344. Lee, C. H.; La, Y.-H.; Park, J.; Park, J. W. *Organometallics* **1998**, *17*, 3648. Nomura, K.; Naga, N.; Takaoki, K. *Macromolecules* **1998**, *31*, 8009.
(8) (a) Galka, C. H.; Trösch, D. J. M.; Rüdenauer, I.; Gade, L. H.; Scowen, I. J.; McPartlin, M. *Inorg. Chem.* **2000**, *39*, 4615. (b) Hellmann, K. W.; Galka, C. H.; Rüdenauer, I.; Gade, L. H.; Scowen, I. J.; McPartlin, M. *Angew. Chem., Int. Ed.* **1998**, *37*, 1948. (c) Hellmann, K. W.; Galka, C. H.; Gade, L. H.; Steiner, A.; Wright, D. S.; Kottke, T.; Stalke, D. *Chem. Commun.* **1998**, 549.
(9) Bazinet, P.; Yap, G. P. A.; Richeson, D. S. *J. Am. Chem. Soc.* **2001**, *123*, 11162.
(10) Bazinet, P.; Yap, G. P. A.; Richeson, D. S. *J. Am. Chem. Soc.* **2003**, *125*, 13314.
(11) (a) Ayers, A. G.; Drost, C. D.; Gehrhus, B.; Hitchcock, P. B.; Lappert, M. F. *Z. Anorg. Allg. Chem.* **2004**, *630*, 2090. (b) Drost, C.; Hitchcock, P. B.; Lappert, M. F. *Angew. Chem., Int. Ed.* **1999**, *38*, 1113.
(12) LaJohn, L. A.; Christiansen, P. A.; Ross, R. B.; Atashroo, T.; Ermler, W. C. *J. Chem. Phys.* **1987**, *87*, 2812.

Table 1. Crystal Data and Structure Refinement for $[(THF)_2Li]_2[1,8\text{-}(^iPrN)_2C_{10}H_6]$ (**1**) and $Sn[1,8\text{-}(^iPrN)_2C_{10}H_6]$ (**2**)

	1	**2**
empirical formula	$C_{32}H_{52}Li_2N_2O_4$	$C_{16}H_{20}N_2Sn$
fw	542.64	359.03
temp (K)	236(2)	238(2)
λ (Å)	0.710 73	0.710 73
space group	$P2_1/n$	$P2_12_12_1$
unit cell dimens		
a (Å)	9.445(5)	9.646(3)
b (Å)	18.168(8)	9.685(3)
c (Å)	19.349(7)	15.689(5)
β (deg)	99.27(3)	
V (Å^3)	3277(3)	1465.7(8)
Z	4	4
density (Mg/m^3) (calcd)	1.098	1.627
abs coeff (mm^{-1})	0.070	1.732
R1[a]	0.0731	0.0596
wR2[b]	0.2058	0.1088

[a] $R1 = \Sigma||F_o| - |F_c||/\Sigma|F_o|$. [b] $wR2 = (\Sigma w(|F_o| - |F_c|)^2/\Sigma w|F_o|^2)^{1/2}$.

Table 2. Selected Bond Distances (Å) and Angles (deg) for $[(THF)_2Li]_2[1,8\text{-}(^iPrN)_2C_{10}H_6]$ (**1**)

Distances			
Li(1)−O(1)	1.991(8)	Li(2)−O(4)	2.000(8)
Li(1)−O(2)	2.041(8)	Li(2)−O(3)	2.107(8)
Li(1)−N(1)	2.007(8)	Li(2)−N(1)	2.020(8)
Li(1)−N(2)	2.024(9)	Li(2)−N(2)	2.029(8)
Li(1)−C(4)	2.632(8)	Li(2)−C(10)	2.677(9)
Li(1)−C(10)	2.684(9)	Li(2)−C(4)	2.710(9)
N(1)−C(4)	1.374(6)	N(2)−C(10)	1.382(6)
N(1)−C(1)	1.462(6)	N(2)−C(14)	1.450(8)
Angles			
O(1)−Li(1)−N(1)	123.2(4)	N(2)−Li(2)−O(3)	124.4(4)
O(1)−Li(1)−N(2)	125.4(4)	N(1)−Li(2)−O(3)	131.2(4)
N(1)−Li(1)−N(2)	86.3(3)	N(1)−Li(2)−N(2)	85.8(3)
O(1)−Li(1)−O(2)	96.2(3)	O(4)−Li(2)−O(3)	91.7(3)
N(1)−Li(1)−O(2)	116.2(4)	O(4)−Li(2)−N(2)	116.6(4)
N(2)−Li(1)−O(2)	111.1(4)	O(4)−Li(2)−N(1)	108.8(3)
C(4)−N(1)−C(1)	116.6(4)	C(10)−N(2)−C(14)	118.6(5)
C(4)−N(1)−Li(1)	100.5(3)	C(10)−N(2)−Li(1)	102.4(4)
C(1)−N(1)−Li(1)	120.9(4)	C(14)−N(2)−Li(1)	120.6(4)
C(4)−N(1)−Li(2)	104.3(4)	C(10)−N(2)−Li(2)	101.8(3)
C(1)−N(1)−Li(2)	122.2(3)	C(14)−N(2)−Li(2)	121.3(5)
Li(1)−N(1)−Li(2)	86.9(3)	Li(1)−N(2)−Li(2)	86.2(3)

atoms were treated as idealized contributions. All scattering factors and anomalous dispersion factors are contained in the SHELXTL 5.1 program library.

Results and Discussion

The direct reaction of diamine $1,8\text{-}(^iPrNH)_2C_{10}H_6$ and MeLi in diethyl ether produced a quantitative yield of $Li_2[1,8\text{-}(^iPrN)_2C_{10}H_6]$ (**1**) which could be purified by crystallization from THF. The spectroscopic analysis of this crystalline product provided a formula indicating incorporation of 4 equiv of THF that we anticipated to be coordinated to the Li cations. Single-crystal X-ray diffraction analysis of these crystals confirmed these features, and the results of this study are presented in Tables 1 and 2 and Figure 1.

Crystallographic characterization of related species is limited to the trimethylsilyl analogues of **A**, $[Li\{(Me_3SiN)_2C_{10}H_6\}\{Li(THF)\}]_2$,[8c] $[\{(HMPA)Li\}_2\{(Me_3SiN)_2C_{10}H_6\}]$[8a] (HMPA = hexamethylphosphoramide), and $[(TMEDA)Li\{(Me_3SiN)_2C_{10}H_6\}_2\{Li_2(\mu\text{-TMEDA})\}]$[8a] (TMEDA = tetramethylethylenediamine), and to one example with neopentyl (Np = $CH_2C(CH_3)_3$) substituents, $[Li\{(NpN)_2C_{10}H_6\}\{Li(THF)\}]_2$.[13] A closely related compound, $\{Li(THF)_2\}_2\{(Me_3SiN)_2C_{10}H_6\}$, has been reported but not structurally characterized.[8c]

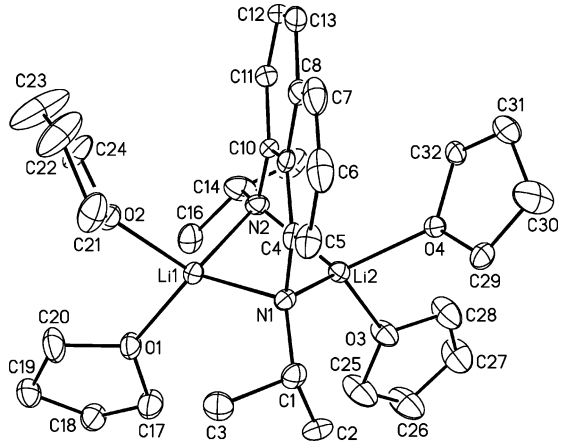

Figure 1. Molecular structure and atom numbering scheme for $[(THF)_2Li]_2[1,8\text{-}(^iPrN)_2C_{10}H_6]$ (**1**). Hydrogen atoms have been omitted for clarity.

Scheme 1

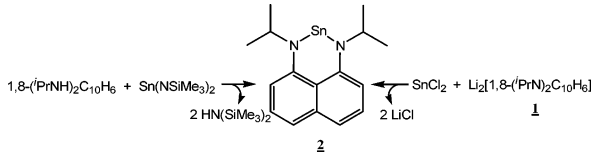

As seen in Figure 1, compound **1** exhibited an approximate C_2 symmetry along the C8−C9 vector. The core of this species is a nonplanar four-membered Li_2N_2 ring (Σ(internal angles) = 345°). Each Li is coordinated to the two amido nitrogens of the DAN ligand, and the four Li−N distances are equal within experimental error. A pseudotetrahedral geometry for each lithium cation is achieved by coordination of two THF molecules to these centers. The ^{i}Pr groups are coplanar with the naphthalene rings displaying torsion angles of 179° (C1−N1−C4−C9) and 177° (C14−N2−C10−C9).

Compound **1** reacts with $SnCl_2$ in diethyl ether to generate $Sn[1,8\text{-}(^iPrN)_2C_{10}H_6]$ (**2**) as a orange/brown solid in excellent yield (Scheme 1). An alternative transamination route employing $Sn(N(SiMe_3)_2)_2$ and the parent diamine released $HN(SiMe_3)_2$ and also yielded **2**. These results parallel our synthesis of $Ge[1,8\text{-}(^iPrN)_2C_{10}H_6]$ (**B**).[9] Compound **2**, although less soluble than the Ge derivative, is soluble in a variety of organic solvents and has been characterized by multinuclear NMR spectroscopy, microanalysis, and a single-crystal X-ray diffraction study. The ^{1}H and ^{13}C NMR spectra of **2** indicate a symmetrical bonding environment for the ligand. Specifically a single set of resonances for the ^{i}Pr groups was observed in the room-temperature spectra. Complex **2** exhibited a resonance in the ^{119}Sn NMR at δ 330 ppm. This falls within the broad range of observed chemical shift values for mononuclear Sn(II) amido compounds. For example the acyclic species $Sn(N(SiMe_3)_2)_2$ displays a ^{119}Sn signal at δ 766 ppm[14] while the cyclic species $1,2\text{-}C_6H_4(NR)_2Sn^{II}$ (**D**) (R = $SiMe_3$, $SiMe_2{}^tBu$) are observed

(13) Danièle, S.; Drost, C.; Gehrhus, B.; Hawkins, S. M.; Hitchcock, P. B.; Lappert, M. F.; Merle, P. G.; Bott, S. G. *J. Chem. Soc., Dalton Trans.* **2001**, 3179.

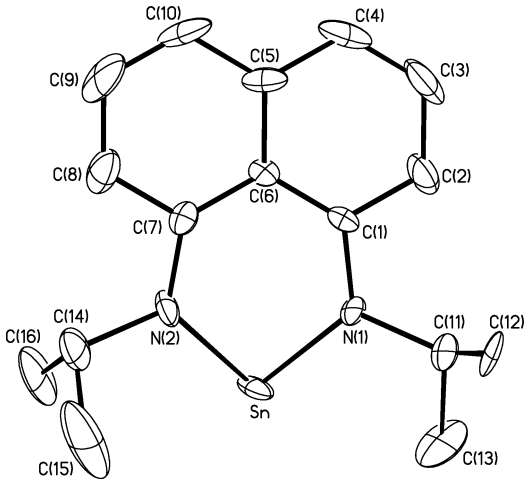

Figure 2. Molecular structure and atom numbering scheme for Sn[1,8-(^{i}PrN)$_2$C$_{10}$H$_6$] (**2**). Hydrogen atoms have been omitted for clarity.

Table 3. Selected Bond Distances (Å) and Angles (deg) for Sn[1,8-(^{i}PrN)$_2$C$_{10}$H$_6$] (**2**)

	Distances		
Sn−N(2)	2.066(8)	N(2)−C(14)	1.53(1)
Sn−N(1)	2.074(8)	C(11)−C(13)	1.53(2)
N(1)−C(1)	1.402(8)	C(11)−C(12)	1.59(2)
N(1)−C(11)	1.51(1)	C(14)−C(15)	1.55(2)
N(2)−C(7)	1.382(9)	C(14)−C(16)	1.579(19)
	Angles		
N(2)−Sn−N(1)	85.6(3)	C(6)−C(1)−N(1)	126.9(4)
C(1)−N(1)−C(11)	119.7(8)	N(2)−C(7)−C(8)	110.2(5)
C(1)−N(1)−Sn	122.9(5)	N(2)−C(7)−C(6)	129.8(5)
C(11)−N(1)−Sn	116.1(7)	N(1)−C(11)−C(13)	111.2(12)
C(7)−N(2)−C(14)	121.0(8)	N(1)−C(11)−C(12)	109.3(10)
C(7)−N(2)−Sn	121.2(5)	C(13)−C(11)−C(12)	111.1(13)
C(14)−N(2)−Sn	117.4(7)	C(15)−C(14)−N(2)	109.4(11)
C(2)−C(1)−N(1)	113.0(4)	C(15)−C(14)−C(16)	109.0(13)

at 415 and 456 ppm with the neopentyl analogue of **D** (R = Np) appearing at δ 269 ppm.[15] The cationic compound **E** displayed a ^{119}Sn NMR signal at 734 ppm,[16] and the closely related derivative **F** (R = Np) appeared at δ 183 ppm.[11b]

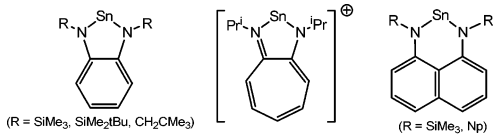

D **E** **F**

Single-crystal X-ray diffraction was used to reveal the structural details of **2** (Table 1), and the results are displayed in Figure 2 with selected bond distances and angles presented in Table 3. As seen in Figure 2, **2** is a mononuclear Sn(II) complex chelated by the dianion [1,8-(N^{i}Pr)$_2$C$_{10}$H$_6$]$^{2-}$. Compound **2** possesses an approximate perpendicular molecular mirror plane of symmetry that bisects the Sn center and contains the C5−C6 vector. The Sn−N bond lengths of 2.066(8) and 2.074(8) Å are identical within experimental error and comparable with the Sn−N bond lengths observed for Sn(N(SiMe$_3$)$_2$ (2.096(1), 2.088(6) Å)[4e] and **D** (R = Np; Sn−N = 2.051(5), 2.067(5) Å).[15] Compound **E** possesses a monoanionic ligand and therefore exhibits slightly longer Sn−N bond lengths (2.153(3), 2.142(3) Å).[16] The most pertinent comparison with **2** is the recently reported structure for the trimethylsilyl congener of **F** (R = SiMe$_3$).[11a] In this species the Sn−N distances are slightly longer at 2.100(5) Å. Also pertinent is the structure of complex **G**, described as the Lewis acid adduct of **F** (R = Np), which displayed Sn−N bond lengths within the Sn(1,8-(NpN)$_2$C$_{10}$H$_6$) fragment that are slightly longer than those of **2** with distances of 2.083(6) and 2.086(6) Å.[11b] As anticipated, the N(1) and N(2) centers in **2** are planar (Σ of angles 358.7 and 359.6°) indicating sp^2 hybridization and the smallest angle around each of the nitrogen atoms is the one defined by the *ipso*-carbon of the ^{i}Pr substituent and the Sn(II) center (117.4(7) and 116.1(7)°).

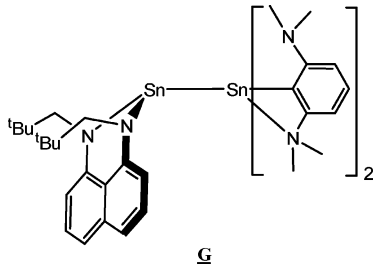

G

Perhaps the most remarkable structural feature of **2** is the pyramidal distortion of the Sn(II) center which lies 0.7688 Å to one side of the N(1)−C(1)−C(6)−C(7)−N(2) plane. The ^{i}Pr substituents deviate to the opposite side of this plane. This feature closely parallels that of the trimethylsilyl analogue of **F** (R = SiMe$_3$) in which the Sn atom lies 0.88 Å out of the plane of the naphthalene group.[11a] These features contrast with the planar five-membered metallaheterocycle structures observed for compounds **D** and **E** and with the planar six-membered cycles observed for the germanium and carbon compounds **B** and **C**. Furthermore, the N(1)−Sn−N(2) angle in **2** of 85.6(3)° is significantly larger than those observed in **D** (R = Np) and **E** with values of 78.5(2) and 74.48(12)°, respectively. In fact, this angle in **2** is comparable to the N−Sn−N angle of 86.9(2)° in **G**. It is also notable that coordination of TMEDA to the Sn(II) center in **D** yields the bimetallic species (TMEDA)[Sn{1,2-(Me$_3$SiN)$_2$C$_6$H$_4$}]$_2$, which exhibits an increased N−Sn−N of 80.9(2)°.[15]

These observations suggested that we examine the extended structure of **2** for features that might help to further explain its structure. This analysis led to the observation of an intermolecular interaction between the Sn center of one molecule with the naphthalene π-electrons of an adjacent compound, which is displayed in Figure 3. The ultimate result of this interaction is the formation of head-to-tail chains of **2** that are aligned along the crystallographic *b* axis. The interaction is not symmetrical with respect to the naphthalene ring, and the shortest intermolecular interactions are observed between Sn and C(3), C(4), and C(5) of a neighboring molecule at distances of 3.022, 2.803, and 3.217 Å, respectively. These distances all fall well within the sum of

(14) Braunschweig, H.; Chorley, R. W.; Hitchcock, P. B.; Lappert M. F. *J. Chem. Soc., Chem. Commun.* **1992**, 1311.
(15) Braunschweig, H.; Gehrhus, B.; Hitchcock, P. B.; Lappert M. F. *Z. Anorg. Allg. Chem.* **1995**, *621*, 1922.
(16) Dias, H. V. R.; Jin, W. *J. Am. Chem. Soc.* **1996**, *118*, 9123.

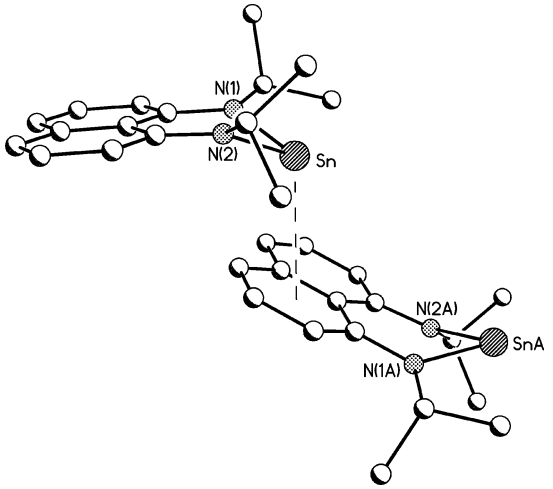

Figure 3. Side view and packing arrangement of Sn[1,8-(^{i}PrN)$_2$C$_{10}$H$_6$] (**2**). The intermolecular interaction described in the text is indicated by a dotted line.

the van der Waals radii of Sn and C of 3.90 Å. For comparison the Sn−C bond in [Sn(CHTMS$_2$)$_2$]$_2$ is 2.22 Å.[17]

It is well established that low-valent p-block metals are capable of forming coordination compounds with aromatic hydrocarbons. These have been most commonly observed for group 13 species, and the interaction has been explained as the overlap of the empty LUMO set of p-orbitals on the metal with the HOMO of the arene.[18] A recent general analysis of crystallographically characterized η^6-arene interactions indicated that there are 9 reported occurrences for Sn(II) and that the ring centroid−Sn distances in these examples fall in the range of 2.45−3.58 Å with an average value of 3.18 Å.[19] Nearly all of these examples involve either η^6-arene interactions with SnC1(AlC1$_4$)[20] or M(AlCl$_4$)$_2$ (M = Sn, Pb).[21] The only directly comparable example in the literature is reported for the neopentyl congener of **D**.[15,22] The extended packing of **D** showed an ordered antiparallel arrangement between adjacent molecules and a short distance between the Sn center of one monomer with the phenylene ring of an adjacent monomeric unit. This interaction was described as a weak η^6-C$_6$H$_4$···Sn interaction leading to dinuclear units with contact between the Sn and the centroid of the phenylene ring of 3.23 Å. Despite the intermolecular interaction, the solid-state structure of **D** displays a planar metallaheterocycle.

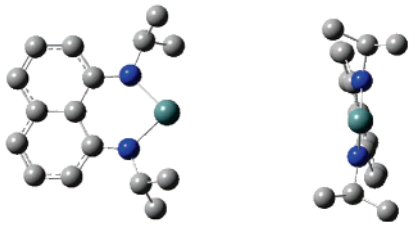

Figure 4. Two views for the optimized structure of Sn[1,8-(^{i}PrN)$_2$C$_{10}$H$_6$] (**2**). The left-hand view is perpendicular to the molecular plane. The right-hand view is along the Sn−C(5)−C(6) axis. Hydrogen atoms have been omitted for clarity.

Table 4. Selected Calculated Structural Parameters for Optimized Sn[1,8-(^{i}PrN)$_2$C$_{10}$H$_6$] (**2**)[a]

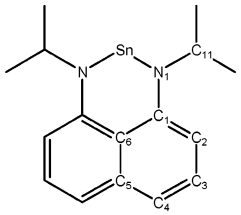

method	PW91PW91/ Sn(AREP),6−311G**	average from expt
Sn−N(1)[b]	2.119	2.07
N(1)−C(1)	1.404	1.39
N(2)−Sn−N(1)[c]	87.9	85.6(3)
C(1)−N(1)−Sn	126.2	122.1
C(11)−N(1)−Sn	115.4	116.8

[a] For ease of comparison with crystallographic data a consistent atom numbering scheme is employed. [b] Distances are in Å units. [c] Angles are in deg.

The structural differences between **D** and **2** may be at least partially attributed to steric effects that arise from the differences in the ligand frameworks of these two species. The symmetrical interaction between the Sn center and the phenylene ring of **D** positions the N-substituents on either side of the aromatic ring with minimal intermolecular steric interactions. In contrast, a similar positioning the Sn center over either of the aromatic rings in the naphthyl backbone of **2** would generate a steric interaction between a substituent on N and the other ring. It appears that the observed structure of **2** minimizes intermolecular steric repulsions through the orientation of the ^{i}Pr groups and the unsymmetrical interaction with the naphthyl group.

To gain additional insight into the origin of the significantly different structure observed for **2** compared to its Ge and **C** analogues and to **D** and **E**, we examined compound **2** computationally by carrying out H-only optimizations on the crystal structure of **2** as well as full optimizations on this compound.[23] Calculations were performed using the PW91[24] method with 6-31G* and 6-311G** basis functions for N, C, and H and averaged relativistic effective core potentials for tin. As a check on the DFT method, a single-point MP2 calculation on the optimized structure was carried out. The results from these calculations are summarized in Figure 4 and Table 4.

(17) Goldberg, D. E.; Hitchcock, P. B.; Lappert, M. F.; Thomas, K. M.; Thorne, A. J.; Fjeldberg, T.; Haaland, A.; Schilling, B. E. R. *J. Chem. Soc., Dalton Trans.* **1986**, 2387.
(18) Schmidbaur, H. *Angew. Chem., Int. Ed. Engl.* **1985**, *24*, 893.
(19) Mascal, M.; Kerdelhue, J.-L.; Blake, A. J.; Cooke, P. A.; Mortimer, R. J.; Teat, S. J. *Eur. J. Inorg. Chem.* **2000**, 485.
(20) Weininger, M. S.; Rodesiler, P. F.; Amma, E. L. *Inorg. Chem.* **1979**, *18*, 751. Schmidbaur, H.; Probst, T.; Huber, B.; Müller, G.; Krüger, C. *J. Organomet. Chem.* **1989**, *365*, 53. Schmidbaur, H.; Probst, T.; Huber, B.; Stelgelmann, O.; Müller, G. *Organometallics* **1989**, *8*, 1567. Schmidbaur, H.; Probst, T.; Steigelmann, O. *Organometallics* **1991**, *10*, 3176.
(21) (a) Weininger, M. S.; Rodsiler, P. F.; Gash, A. G.; Amma, E. L. *J. Am. Chem. Soc.* **1972**, *94*, 2135. (b) Gash, A. G.; Rodesiler, P. F.; Amma, E. L. *Inorg. Chem.* **1974**, *13*, 2429. (c) Rodesiler, P. F.; Auel, T.; Amma, E. L. *J. Am. Chem. Soc.* **1976**, *97*, 7405. Lefferts, J. L.; Hossain, M. B.; Molloy, K. C.; Van der Helm, D.; Zuckerman, J. J. *Angew. Chem., Int. Ed. Engl.* **1980**, *19*, 309.
(22) An example of a π interactions between Sn(II) imido clusters leading to extended aggregations is reported in the following: Bashall, A.; Ciulli, A.; Harron, E. A.; Lawson, G. T.; McPartlin, M.; Mosquera, M. E. G.; Wright, D. S. *Dalton Trans.* **2002**, 1046.

Table 5. Calculated Energy Difference between the Optimized Structures of Sn[1,8-(^{i}PrN)$_2$C$_{10}$H$_6$] (**2**) and the Experimentally Observed Structure from Single-Crystal X-ray Analysis

method	PW91PW91/ Sn(AREP),6-31G*	MP2/Sn(AREP),6-31G*// PW91PW91/Sn(AREP),6-31G*	PW91PW91/ Sn(AREP),6-311G**
energy diff (kcal/mol)	−25.3	−23.9	−23.9

The full structure optimizations yielded molecular structures with the Sn center lying in the plane of the naphthyl group and with only a slight twist in the metallaheterocycle (Figure 4). These structures exhibit the symmetrical features suggested by the NMR spectroscopic measurements on **2** and which are similar to the reported structures of **B**, **D**, and **E**. However, these structures differ considerably from the solid-state crystallographic data obtained for **2**. The optimized structures exhibited calculated energy values that are consistently 24 kcal/mol lower than the calculated single point energies for the pyramidal structure that is observed experimentally (Table 5). The large calculated energy difference between the X-ray and gas-phase structures lends strong support to the idea that the X-ray structure is distorted from the ideal molecular geometry. We performed an additional calculation using MP2/6-311G** on the structure shown in Figure 3, wherein the monomer structures were constrained to that obtained from the X-ray crystal structure. We were unable to perform full geometry optimizations at this level of theory. However, the result indicates that a substantial portion (16.6 kcal/mol) of the deformation energy of the monomer is recovered through dimer formation. It is likely that a more detailed theoretical treatment would show that the distortion of **2** to a tetrahedral geometry is required for polymer formation.

We attribute the observed geometry of **2** to the donation of the π-electrons of the naphthalene moiety to a Lewis acidic Sn center which in turn leads to the supramolecular head-to-tail chains that are described above. Our description is supported by the documented interactions of species **D**,[15] **E**,[16,25] and **F**[11] with Lewis bases. We have found additional support for this proposition in the recently reported structure of **F** (R = $SiMe_3$).[11a] Our examination of the crystal packing of this species revealed unreported intermolecular interactions with the shortest contacts being observed between one Sn center and three naphthalene ring carbons (positions 3−5) of a neighboring molecule at distances of 3.092, 2.777, and 3.168 Å. As with complex **2** the ultimate result of these interactions is formation of chains in the extended structure of this compound.

Conclusions

Our application of *N*,*N*′-diisopropyl-1,8-diaminonaphthalene ligands has been extended to the preparation of the cyclic diamidostannylene **2**. This compound, unlike its lighter element analogues, exhibits a nonplanar metallaheterocycle in the solid state. The origin of this deviation is due to intermolecular Lewis acid/base Sn···arene interactions that in turn lead to the formation of head-to-tail chains in the extended structure. Computational studies support the fact that a planar geometry is energetically favored by 24 kcal/mol, a feature that is consistent with the solution NMR spectroscopy data. The observed pyramidal distortion of the metallaheterocycle is a recurring motif among related compounds employing diaminonaphthalene-derived ligands. The Lewis acid behavior of these Sn(II) species contrasts with the well-documented behavior of the lighter congeners of group 14 to function as Lewis bases.

Acknowledgment. This work was supported by the Natural Sciences and Engineering Research Council of Canada.

Supporting Information Available: Crystallographic information files (CIF) for compounds **1** and **2** and the coordinates of the optimized structures of compound **2**. This material is available free of charge via the Internet at http://pubs.acs.org.

IC050238U

(23) Frisch, M. J.; Trucks, G. W.; Schlegel, H. B.; Scuseria, G. E.; Robb, M. A.; Cheeseman, J. R.; Montgomery, J. A., Jr.; Vreven, T.; Kudin, K. N.; Burant, J. C.; Millam, J. M.; Iyengar, S. S.; Tomasi, J.; Barone, V.; Mennucci, B.; Cossi, M.; Scalmani, G.; Rega, N.; Petersson, G. A.; Nakatsuji, H.; Hada, M.; Ehara, M.; Toyota, K.; Fukuda, R.; Hasegawa, J.; Ishida, M.; Nakajima, T.; Honda, Y.; Kitao, O.; Nakai, H.; Klene, M.; Li, X.; Knox, J. E.; Hratchian, H. P.; Cross, J. B.; Bakken, V.; Adamo, C.; Jaramillo, J.; Gomperts, R.; Stratmann, R. E.; Yazyev, O.; Austin, A. J.; Cammi, R.; Pomelli, C.; Ochterski, J. W.; Ayala, P. Y.; Morokuma, K.; Voth, G. A.; Salvador, P.; Dannenberg, J. J.; Zakrzewski, V. G.; Dapprich, S.; Daniels, A. D.; Strain, M. C.; Farkas, O.; Malick, D. K.; Rabuck, A. D.; Raghavachari, K.; Foresman, J. B.; Ortiz, J. V.; Cui, Q.; Baboul, A. G.; Clifford, S.; Cioslowski, J.; Stefanov, B. B.; Liu, G.; Liashenko, A.; Piskorz, P.; Komaromi, I.; Martin, R. L.; Fox, D. J.; Keith, T.; Al-Laham, M. A.; Peng, C. Y.; Nanayakkara, A.; Challacombe, M.; Gill, P. M. W.; Johnson, B.; Chen, W.; Wong, M. W.; Gonzalez, C.; Pople, J. A. *Gaussian 03*, revision B.04; Gaussian, Inc.: Wallingford, CT, 2004.

(24) Burke, K.; Perdew, J. P.; Wang, Y. In *Electronic Density Functional Theory: Recent Progress and New Directions*; Dobson, J. F., Vignale, G., Das, M. P., Eds.; Plenum Press: New York, 1998. Perdew, J. P. In *Electronic Structure of Solids*; Ziesche, P., Eschrig, H., Eds.; Akademie Verlag.: Berlin, 1991; Vol. 91.

(25) Ayers, A. E.; Dias, H. V. R. *Inorg. Chem.* **2002**, *41*, 3259.